



## Interactions between demersal fish body condition and density during the regime shift of the Gulf of Lions

Cyria Meriem Bensebaini, Grégoire Certain, Norbert Billet, Angélique Jadaud, S. Gourguet, Tarek Hattab, Jean-Marc Fromentin

### ► To cite this version:

Cyria Meriem Bensebaini, Grégoire Certain, Norbert Billet, Angélique Jadaud, S. Gourguet, et al.. Interactions between demersal fish body condition and density during the regime shift of the Gulf of Lions. ICES JOURNAL OF MARINE SCIENCE, 2022, 10.1093/icesjms/fsac106 . hal-03718440

**HAL Id: hal-03718440**

**<https://hal.umontpellier.fr/hal-03718440>**

Submitted on 9 Jul 2022

**HAL** is a multi-disciplinary open access archive for the deposit and dissemination of scientific research documents, whether they are published or not. The documents may come from teaching and research institutions in France or abroad, or from public or private research centers.

L'archive ouverte pluridisciplinaire **HAL**, est destinée au dépôt et à la diffusion de documents scientifiques de niveau recherche, publiés ou non, émanant des établissements d'enseignement et de recherche français ou étrangers, des laboratoires publics ou privés.

## Interactions between demersal fish body condition and density during the regime shift of the Gulf of Lions

Bensebaini Meriem <sup>1,\*</sup>, Certain Gregoire <sup>1</sup>, Billet Norbert <sup>1</sup>, Jadaud Angelique <sup>1</sup>, Gourguet Sophie <sup>2</sup>, Hattab Tarek <sup>1</sup>, Fromentin Jean-Marc <sup>1</sup>

<sup>1</sup> UMR 9190 MARBEC, University of Montpellier-IRD-Ifremer-CNRS , Av. Jean Monnet, CS 30171, Sète Cedex 34203, France

<sup>2</sup> UMR 6308 AMURE, University of Brest-Ifremer, CNRS-IUEM , Rue Dumont d'Urville 29280 Plouzané, France

\* Corresponding author : Meriem Bensebaini, email address : [bensebaini.cyria@gmail.com](mailto:bensebaini.cyria@gmail.com)

### Abstract :

Environmentally driven changes in small pelagic fish condition and size have been observed in the Gulf of Lions (GOL) since 2008, leading to a significant fishery crisis. However, the effect of changes in environment and/or in the small pelagic community on the demersal community remain unknown. For the first time, this study examines the body condition (bc) and population density of 22 demersal species since 1994, using dynamic factor analysis (DFA). Most (but not all) of demersal species have shown a common shift between 2006 and 2009, which is synchronous with that observed in small pelagic species and the environmental conditions in the GOL. It had been concluded that the environmentally driven changes detected in the pelagic fish community also affected the demersal fish community, but with less drastic and lasting consequences. As the DFA revealed that the bc displayed important variations for several species, notably hake (*Merluccius merluccius*), the interaction between the bc and population density was investigated using the Multivariate Autoregressive (MAR) model on hake population at three life stages (recruits, juveniles, and adults). Results showed that adult bc, while negatively affected by density, had a positive effect on recruitment. So hake bc could have affected population dynamics by promoting higher recruitment at low densities. Further work is needed to ascertain whether such effects exist in other demersal species.

**Keywords :** body condition, demersal fish, dynamic factor analysis, Gulf of Lions, *Merluccius merluccius*, multivariate autoregressive models

## 28    **Introduction**

29    The Gulf of Lions (GOL) is one of the most productive regions of the Mediterranean Sea, due to its  
30    wide continental shelf and a combination of large inflows from the Rhone River and small-scale  
31    coastal upwelling (Millot, 1982, 1990). This area has been intensively exploited for decades, with

total landings reaching 30,000 to 50,000 tonnes from the 1970s to the 1990s, but only amounting to 13,604 tonnes (tuna excluded) in 2018 (STECF, 2019a, 2019b). Today, fish stocks of commercial interest are heavily overfished, according to the report of the State of Mediterranean and Black Sea Fisheries (SoMFi) (FAO, 2018a). It is therefore a high-stakes sector from an ecological, social and economic perspective, where the consequences of unexpected changes could be considerable (Barange *et al.*, 2018).

Around 2008, the pelagic ecosystem of the GOL had shown signs of disruption, characterized by the drastic changes in size, age and condition of its two main small commercial pelagic fish stocks (European sardine, *Sardina pilchardus*; European anchovy, *Engraulis encrasicolus*). This “small pelagic crisis” in the GOL was attributed to slower growth and higher natural mortality in the older age groups (Van Beveren *et al.*, 2014). Different hypotheses about the causes of such changes have been tested and finally seemed to result from a bottom-up control induced by a change in plankton composition and/or density (Brosset *et al.*, 2015; Saraux *et al.*, 2019). Subsequent studies indicated that environmental conditions in the GOL broadly changed in the mid-2000s (Feuilloley *et al.*, 2020). These types of large-scale disturbances are known for their effects on fish species biology, directly – physiological threshold – or indirectly – by modifying the food resource (plankton), thereby affecting bottom-up mechanisms (Jørgensen, 1992). This has consequences on the energy storage dynamics of individuals (Jakob *et al.*, 1996), reflected in their body condition (BC), and ultimately in their natural mortality and growth, affecting population dynamics. Fluctuations in population density and BC therefore provide information on population health. The small pelagic crisis first induced a crash in landings, followed by a historic collapse of the fishing activity in the area (Van Beveren *et al.*, 2016) and the shift of fishing efforts towards demersal stocks, which increased an already unsustainable fishing pressure on the demersal species. As such, the demersal stocks became crucial for the survival of the trawl and small-scale fisheries in the region. The captures during the decade preceding the crisis (outside of tuna catches) were composed of around 3/4 of small pelagic species, mainly sardine and anchovy, and around 1/4 of demersal species, while post-crisis (after 2008) the pattern reversed to 1/3 of small pelagic species and almost 2/3 of demersal species (FAO, 2018b).

While the small-pelagic shift of the GOL has been the center of an intense research activity (summarized in Saraux *et al.* 2019), not much has been done to discover whether demersal stocks have also been affected, since studies on demersal species’ BC in the GOL are over a decade old (Lloret *et al.*, 2002, 2008; Ferraton *et al.*, 2007). Similar changes in BC are likely to be observed in the demersal community, especially since many demersal species depend on environmental conditions when they are in a larval or juvenile stage, and, once adult, certain demersal species feed mainly on small pelagic fishes (Banaru *et al.*, 2013; Mellon-Duval *et al.*, 2017). BC can have a strong

66 impact on growth (Ratz and Lloret, 2003) and natural mortality, as fish in poor condition are more  
67 susceptible to disease, predation, and fishery (Martinez *et al.*, 2003). BC can also affect reproduction  
68 or reproductive potential, which is crucial for the recovery of a declining stock. Some fish populations  
69 in poor condition invest their energy in growth rather than reproduction, reducing fecundity and the  
70 quality of the eggs, or leading to delayed maturation (Lambert and Dutil, 2000; Lloret *et al.*, 2008),  
71 while others, such as small pelagic fish in the GOL, continue their energy investment in reproduction,  
72 whatever their BC, leading to an increased mortality after spawning (Brosset *et al.*, 2016). The search  
73 for possible links between BC and population dynamics is therefore interesting.

74 This paper has two goals. First, we explore the demersal species' response to an ecosystem shift  
75 detected in the GOL around 2008. Then, we investigate the population dynamics of a highly  
76 documented species, the European hake (*Merluccius merluccius*), to better understand how BC and  
77 density interact at a population level. Hence, the first part of the paper is dedicated to determining  
78 whether the BC and/or density of demersal species has changed over time. More precisely, we have  
79 looked for common trends between 22 demersal species (in terms of BC and density) and investigated  
80 if these common trends match those already detected by Feuilletoley *et al.* (2020) in the environmental  
81 conditions and small pelagic fish species of the GOL. In the second section, we use the European  
82 hake as a study model to examine to what extent changes in BC and/or density could affect one  
83 another, using Multivariate Autoregressive (MAR) models. The choice of hake was mostly motivated  
84 by its central role in the demersal fishery (Mellon-Duval *et al.*, 2017) and by data availability. Hake  
85 was the only species which had enough information available to set up a three-stage population  
86 dynamics model suitable for searching for interactions between BC and the density of hake at various  
87 stages (recruits, juveniles, and adults).

88 With this study, we hope to uncover crucial information that helps provide a better understanding of  
89 the dynamics of the demersal stocks in the GOL, and ultimately contribute to the establishment of a  
90 more ecosystem-oriented approach to fisheries management in this area.

## 91 **Materials and methods**

### 92 **Data description: The MEDITS survey**

93 Data used in the analyses were collected from annual international bottom trawl surveys performed  
94 in May-July since 1994 over the continental shelf (10 m to 200 m depth) and the continental slope  
95 (200 m to 800 m) of the Mediterranean Sea through the MEDITS scientific program (Bertrand *et al.*,  
96 2002). The sampling procedures were standardized according to a common protocol over countries  
97 and years. The MEDITS survey (Jadaud, 1994) aims to annually estimate and monitor the demersal  
98 fish stocks in the GOL and east of Corsica. The current study focuses on the GOL (Figure 1). The  
99 fishing gear used is a bottom trawl GOC-73 with 20 mm of stretched cod-end mesh size. The average

vertical and wing opening of the gear are around 2 m and 18 m, respectively. All the tows were performed during daylight hours, 30 min for shelf stations, and 60 min for the continental slope. The MEDITS database documents the distribution and density of roughly 400 Mediterranean species collected over 25 years of sampling. However, for many reasons such as a lack of data or appropriate biological measurements throughout the whole time series (see e.g. Morfin *et al.*, 2012), we restricted our analysis to 22 species that were regularly caught (i.e. there were no missing values in the time series) during the survey and for which length measurements were consistently taken during the whole time period (see Table 1). The survey provides the population density for each species, obtained by dividing the number of individuals of each species obtained in any given trawl by the trawled surface (the annual densities being the average of all densities obtained in any given year for each species, see Supplementary Figure S1). Density is here used as a proxy of abundance in the GOL relative to the trawl catchability, which is assumed to be constant through time, since the fishing protocol has carefully been kept constant since 1994 (Morfin *et al.*, 2012).

### Body condition index

To measure the BC, the residual index (Gould, 1975) was used, which is the residual of the length-weight log-linear relationship. Positive residuals indicate the BC is above average, while negative residuals indicate the BC is below average. This index is convenient as it allows to separate the BC from the body size effect (Jakob *et al.*, 1996).

The MEDITS protocol includes systematic measurements of individual size for the 22 selected species, but few of them are individually weighed. In the absence of individual weights for each species and in each haul sample, the data available consists of a total biomass and an associated size spectrum. However, it is still possible to estimate a length-weight relationship from these data. The classical length-weight relationship is written as follows:

$$w_{s,i} = a_s l_{s,i}^{b_s} \dots \dots \dots (1)$$

The  $w_{s,i}$  and  $l_{s,i}$  are the weight and length of individual  $i$  of species  $s$ , respectively. The total biomass in one haul  $h$  of a given species  $s$ , thereafter denoted  $B_{h,s}$ , is equal to the sum of the  $n$  individuals' weight ( $w_i$ ) contained in the haul  $h$ , as described in equation (2).

$$B_{h,s} = \sum_{i=1}^n w_{h,s,i} = a_s \sum_{i=1}^n l_{h,s,i}^{b_s} \dots \dots \dots (2)$$

Where  $B_{h,s}$  is the observed biomass of species  $s$  in the  $h^{\text{th}}$  haul and  $a_s$  and  $b_s$  are the typical constants of the length-weight relationship of the given species  $s$ , and  $l_{h,s,i}$  is the length of the  $i^{\text{th}}$  fish in the  $h^{\text{th}}$  haul of the species  $s$ .

The number of hauls varies slightly from year to year (the average number being 65). To calculate the residual index based on the same number of hauls each year and produce confidence intervals, the residual index time series were extracted using 100 non-parametric bootstraps. For each species

134 and bootstrap, 40 hauls were randomly selected each year, resulting in a 1000-point data set (40 haul  
135 \* 25 years). Then the estimates of parameters  $a_s$  and  $b_s$  were obtained by fitting the equation (2) to  
136 the 1000 pairs of  $B_{h,s}$  and their corresponding sum of sizes, then finally, residuals were calculated  
137 from the fit of the equation (2). Averaging these residuals per year for each bootstrap sample resulted  
138 in 100 time series of 25 years, from which the median – and 2.5% and 97.5% quantiles for confidence  
139 intervals – were extracted to build the BC index series for each species. These steps are described  
140 graphically in Figure 2 and the BC time series can be consulted in Supplementary Figure S2.  
141 Furthermore, to check for consistency, bootstrapped estimates of  $a_s$  and  $b_s$  parameters were compared  
142 to parameters from the bibliography, and the obtained results were satisfactory (Supplementary Table  
143 S1).

144 **Dynamic Factor Analysis (DFA)**

145 DFA is a dimension reduction technique specifically designed for time series since it takes into  
146 account the time factor, unlike other dimension reduction techniques like principal component  
147 analysis (PCA) or canonical correspondence analysis (CCA). DFA aims to identify common trends  
148 between different time series and relationships between these series (Zuur *et al.*, 2003). It fits linear  
149 multivariate autoregressive state-space models with Gaussian errors (Holmes *et al.*, 2018). The model  
150 is written as follows:

151 
$$y_t = Zx_t + v_t \text{ where } v_t \sim MVN(0, R) \dots\dots\dots (3a)$$

152 
$$x_t = x_{t-1} + w_t \text{ where } w_t \sim MVN(0, Q) \dots\dots\dots (3b)$$

153 The  $y$  equation (3a) represents the observation process, and the  $x$  equation (3b) is termed the state  
154 process. The vector  $y_t$  of  $n$  time series (corresponding to the number of analyzed species,  $n=22$ ) is  
155 modeled as a linear combination of  $m$  hidden common trends ( $x_t$  vector) and the factor loadings matrix  
156  $Z$ , and observation errors vector  $v_t$ , which were distributed as a multivariate normal distribution with  
157 mean vector 0 and variance-covariance matrix  $R$ . The  $m$  hidden common trends at time  $t$  ( $x_t$ ) follow  
158 random walks with process error vector  $w_t$ , which was distributed as a multivariate normal distribution  
159 with mean vector 0 and variance-covariance matrix  $Q$  (Holmes *et al.*, 2018). For any given time  $t$  and  
160 species  $s$ , the linear form of the model can be written as follows:

161 
$$y_{st} = z_{s1}x_{1t} + z_{s2}x_{2t} + \dots\dots + z_{sm}x_{mt} + v_{st} \dots\dots\dots (4)$$

162 Two DFA were carried out, one for the BC time series and another for the density time series. In both  
163 cases, several models were fitted, which had from  $m=1$  to  $m=3$  latent variables, and a covariance  
164 matrix  $R$  starting from its simplest form “diagonal and equal” (i.e. the same variance and no  
165 covariance) to a more complex form “equalvarcov” (i.e. one value for the variance and one for the  
166 covariance). Model selection was based on Akaike’s information criterion for small samples (AICc;

167 Burnham and Anderson, 2002) to identify the most parsimonious model containing the least number  
168 of common trends without experiencing much information loss. The Multivariate Autoregressive  
169 State-Space (MARSS) package developed in *R* (Holmes *et al.*, 2018; R Core Team, 2020) was used  
170 to perform these analyses. As input data for the DFA, we used log-transformed and centered density,  
171 and standardized BC time series.

172 Trends identified by this DFA analysis were then compared to the time series retrieved from the study  
173 by Feuilleley *et al.* (2020). These authors investigated whether an environmental change could have  
174 triggered the small pelagic crisis based on two DFA analyses, one including the time series of 10  
175 biological variables (biomass, condition and size for sardine, anchovy and sprat plus abundance for  
176 sardine) and one including the time series of 10 environmental variables (chlorophyll-a (Chla)  
177 concentration, Rhone flow, thermal fronts, Sea Surface Temperature (SST), Western Mediterranean  
178 Oscillation Index, convection, upwelling, stratification index, N and P nutrient concentration). These  
179 two DFA analyses revealed common trends with a shift in the mid-2000's, which led the authors to  
180 suggest that changes in environmental conditions could have affected plankton production and hence  
181 the small pelagic fish community (Feuilleley *et al.*, 2020). Those two common trends have been thus  
182 retrieved and compared with the results of the DFA analyses carried out in this study on the demersal  
183 community to investigate a potential match between trends in environment, small pelagic and  
184 demersal fish communities in the GOL.

### 185 **Multivariate Autoregressive (MAR) Model**

186 This part of the study looks for interaction between BC and density, using the Granger causality (GC)  
187 concept (Granger, 1969). The basic idea of GC is that a variable  $x$  impacts a variable  $y$  if it improves  
188 the prediction of the latter. This concept can be based on the fitted interaction matrix obtained from  
189 a MAR model (Ives *et al.*, 2003; Certain *et al.*, 2018). MAR(p) models, in their linear formula, have  
190 demonstrated a particular efficiency in detecting interactions in nonlinear systems (Barraquand *et al.*,  
191 2021). This analysis was based on a conditional GC (Geweke, 1984; Barnett and Seth, 2014), in  
192 which, when focusing on the causal relationship between two variables, the confounding relationships  
193 are accounted for due to the remaining variables.

194 We focused on European hake because: (i) it is a well-sampled species and the most documented of  
195 the MEDITS survey; (ii) its life cycle is well known and the timing of the MEDITS survey (late spring)  
196 has been designed to capture hake recruitment; (iii) it is one of the most important and abundant  
197 species of the demersal community in the GOL; (iv) it is a major commercial species; and (v) its BC  
198 increased significantly through the study period. European hake is widely distributed in the GOL,  
199 with juvenile and young adults concentrated mainly on the continental shelf, and the largest  
200 individuals deeper on the slope and canyons (Maynou *et al.*, 2003). Hake is a key predator in this



201 area, feeding mainly on crustaceans and small benthic fish when juvenile, then switching to a more  
202 piscivorous diet at 15 cm (small pelagics and blue whiting representing 40% to 80% of its diet,  
203 Mellon-Duval *et al.*, 2017). It is a highly mobile species, with long lifespan and slow growth (Mellon-  
204 Duval *et al.*, 2010). The European hake is a batch spawner that spawns throughout the year with a  
205 peak in winter (Ferrer-Maza *et al.*, 2014), and recruitment also happens throughout the year with a  
206 peak in late spring. Juveniles are fished as soon as they reach a catchable size (i.e. in their first year  
207 of life).

208 A MAR(1) analysis was done using density and BC as variables. Both the BC and density were split  
209 into three stages using an age-length key (Bensebaini *et al.*, 2019): juveniles (or recruits) age 0-1;  
210 juveniles age 1-2; and adults age 2+ (Supplementary Figure S3). Separating adults from juveniles  
211 permits the verification of whether maturation and modifications in physiological processes, leading  
212 to changes in the body's energy resources management (Kooijman, 2009), affects the BC-density  
213 relationship. In addition, natural mortality is higher in juveniles – which are more vulnerable to  
214 predation compared to adults (Vetter, 1988) – and possibly act as a confounding factor. Recruits  
215 (juveniles age 0-1) were separated from other juveniles (juveniles age 1-2) in an attempt to acquire  
216 recruitment dynamics. The MAR analysis was restricted to a one-year lag due to the shortness of the  
217 time series (i.e. 25 points), as increasing the lag also greatly increases model dimensionality.

218 In matrix form, MAR models with one time lag (MAR (1) models) are written as follows:

219 
$$x_t = Bx_{t-1} + w_t \text{ where } w_t \sim MVN(0, Q) \dots\dots\dots (5)$$

220 with  $x_t$  a vector whose elements corresponds to the response variables of the model; either total log-  
221 density or BC, each being divided by three stages.  $B$  is the 6\*6 interaction matrix, with  $b_{ij}$  the effect  
222 of variable  $j$  on variable  $i$ . The diagonal of the matrix  $B$  represents the effect of the variables on  
223 themselves.  $w_t$  is a multivariate normally distributed error vector with mean 0 and variance-  
224 covariance matrix  $Q$ . Matrix  $B$  parameters were estimated by a maximum likelihood estimation using  
225 a Kalman filter (Harvey, 1989). Each parameter was considered significant with a p-value lower than  
226 a significance level of 5% and was associated with a 95% confidence interval.

227 Considering the high number of parameters to be estimated in the full model and the relatively short  
228 length of the available time series, we designed a specific approach to avoid a potential overfitting  
229 issue. To do so, we first set all parameters that had no biological meaning (see Supplementary Table  
230 S2) to 0, such as  $b_{14}$ , because the BC of the recruits at time  $t$  cannot affect the density of recruits at  
231 time  $t+1$  (since the latter are not yet born, see Supplementary Table S3). Then, backward elimination  
232 was based on the AICc to keep the most relevant coefficients and to penalize overly complex models.  
233 However, some coefficients related to the population dynamics have not been included in the

234 backward elimination because of their key biological meaning:  $b_{21}$  and  $b_{32}$  (i.e. the growth in density  
235 of recruits age 0-1 and of juveniles age 1-2, respectively) as juveniles age from one year to the next;  
236  $b_{13}$  (i.e. the adults reproductive output) because adults reproduce and give birth to recruits; and  $b_{33}$   
237 (i.e. density-dependent effects within the adult density) because adult density cannot grow  
238 indefinitely.

239 Because the aim of this study is to determine whether recruit density is better predicted with an adult  
240 BC effect, The sum of squares of residuals (SSR) of recruit density were computed and compared for  
241 the models with and without the effect of adult BC on recruit density.

## 242 Results

### 243 DFA

244 For the BC, the AICc (Supplementary Table S4) selected two models as the most parsimonious  
245 ( $\Delta AICc=1.9$ ). One contained one common trend and an “equalvarcov” covariance matrix R (i.e. a  
246 common variance for all series and common covariance between them), and the other contained two  
247 common trends, and an “equalvarcov” covariance matrix R. Both models were tested and showed  
248 similar results. However, the model with a common trend (Supplementary Figure S4) had lower factor  
249 loadings, probably because a single common trend was insufficient to properly describe the common  
250 dynamics of demersal fish BC, which forms the rationale for the selection of the model with two  
251 common trends (Figure 3). The first common trend showed a sharp drop in 1994, then a gradual  
252 increase from 2006 to 2016. The second common trend displayed a typical regime shift pattern: it  
253 dropped sharply between 2006 and 2009, after which it remained below zero until the end of the  
254 series. Species with factor loadings (Figure 3) smaller than a threshold of 0.2, in absolute values, have  
255 not been included in the interpretation of results (Zuur *et al.*, 2003), as they did not have a particular  
256 trend over time. Factor loadings resulting from the DFA on BC (Figure 3) seemed clustered by  
257 taxonomic categories, suggesting that the BC of species within a taxonomic group followed a similar  
258 temporal dynamics. Cephalopods (three species) mainly displayed negative loadings on trend 2, while  
259 perciforms (five species) and John dory displayed positive loadings on trend 2. Pleuronectiforms (two  
260 species) were mostly positively associated with trend 1, while gadiforms (four species) and  
261 scorpaeniforms (two species) were positively associated with both trends 1 and 2, except hake, which  
262 only displayed positive loadings on trend 1. Lophiiforms (two species) were poorly associated with  
263 both trends.

264 When looking at the overall model fits for each BC time series (Supplementary Figure S5), most  
265 species showed a good fit with the observations, except for a few species (Norway lobster,  
266 blackbellied angler, red mullet, and blackspot seabream series). As several species were associated  
267 with both common trends, the contribution of each BC time series to the two common trends was  
268 plotted in different colors (Figure 4) to determine at which point in the series the model was more  
269 driven by trend 1 or 2. In the shift period (2006-2009), almost all species were driven by trend 2 (i.e.  
270 blue points) except for European hake, spotted flounder, and angler, whose BCs were only associated  
271 with trend 1 (Figure 3).

272 For density, the AICc (Supplementary Table S5) selected the model containing one common trend,  
273 and an “equalvarcov” covariance matrix R. This common trend (Figure 5) showed low values until  
274 2006, then values quickly increased until 2010, and finally the increase slowed until it reached what  
275 appears to be a plateau in 2014. Again, species with factor loadings smaller than 0.2 were not included

276 in the interpretation of results (bottom part of Figure 5 for factor loading; and Supplementary Figure  
277 S6 for density model fits versus observed time series), leaving only shortfin squid and three  
278 perciforms (blackspot seabream, common pandora, and Mediterranean horse mackerel), which were  
279 positively associated with this trend, while blue whiting was negatively associated with it.

280 The common trend from DFA on demersal fish densities, the trend 2 from the DFA on demersal fish  
281 BC and the common trends of the DFA analyses on environmental conditions and small pelagic fishes  
282 in the GOL performed by Feuilloley *et al.* (2020) are displayed in Figure 6. This figure highlights a  
283 strikingly concomitant period of shift (2006-2009), when the strongest changes in these four trends  
284 occurred.

### 285 **Multivariate Autoregressive (MAR) Model**

286 The model selected by backward elimination is illustrated in Figure 7. Results show that coefficients  
287 that have not been included in the backward elimination ( $b_{21}=0.01\pm0.32$ ,  $b_{32}=0.12\pm0.40$ ,  
288  $b_{33}=0.1\pm0.48$ ) were low and not statistically significant, except  $b_{13}$ , which revealed the strong positive  
289 effect of the density of adults age 2+ at time  $t$  on recruits age 0-1 at time  $t+1$  ( $b_{13}=0.90\pm0.46$ ). The  
290 density of adults age 2+ at time  $t$  also had a negative effect on the BC of juveniles age 1-2 ( $b_{53}=-$   
291  $0.22\pm0.14$ ), and adults age 2+ ( $b_{63}=-0.33\pm0.2$ ) at time  $t+1$ . Finally, the BC of adults age 2+ had a  
292 positive effect ( $b_{16}=0.83\pm0.69$ ) on the density of recruits age 0-1 at time  $t+1$  and was negatively  
293 autocorrelated ( $b_{66}=-0.36\pm0.29$ ). The calculation of the SSR shows that there was a reduction of the  
294 SSR in the model with the effect of the BC, as compared with the model without this effect (a  
295 reduction of 17.20%). This means that juvenile density was better predicted when accounting for the  
296 BC.

## 297 Discussion

298 One of the first goals of this study was to explore whether the environmentally driven changes in  
299 small pelagic fish BC could also be detected in the demersal fish community of the GOL. DFA  
300 performed on the BC and density time series of 22 demersal species tended to confirm this impact.  
301 This was documented by a common shift between 2006 and 2009 for most (but not all) demersal  
302 fishes and a striking synchrony between the common trends extracted from the DFA of this study (on  
303 demersal fish) and those performed on the small pelagic fishes and environmental conditions in the  
304 GOL (Feuilloley *et al.*, 2020). The authors have clearly depicted an overall change in the  
305 environmental conditions of the GOL over the last 30 years, characterized by a rapid decline in Chla  
306 concentration in the mid-2000s, a continuous increase in SST, an intensification of coastal upwellings  
307 and frontal activities, a decrease in the nutrient inputs from the Rhone river as well as in the deep  
308 winter convection and modifications in the regional atmospheric conditions (as described by the  
309 Western Mediterranean Oscillation Index). Those environmental changes have probably affected the  
310 lower trophic levels (plankton) of the GOL ecosystem, and consequently the small pelagic fish  
311 compartment, as already stressed by previous studies (see Saraux *et al.*, 2019; Brosset *et al.*, 2015).  
312 The present study shows that these environmental changes may also have affected the demersal fish  
313 community. However, the exact cause and pathways of these changes are yet to be discovered. Hence,  
314 the processes through which environmental changes might have affected energy storage and fish BC  
315 will probably remain a challenging research topic for the next decade, requiring more theoretical  
316 approaches before it is solved.

317 The BC of many demersal species were both positively correlated with trend 1 (a continuous BC  
318 improvement) and with trend 2 (the shift in the mid-2000s). For these species, the contribution of  
319 trend 2 is substantial during the shift period (blue points in fig 4), while the contribution of trend 1 is  
320 more significant at the end of the time series. Hence the BC of these species (blue whiting, greater  
321 forkbeard, capelan, Mediterranean and Atlantic horse mackerel, grey gunnard, blackbelly rosefish  
322 and John dory), while momentarily altered during the shift, saw an improvement in recent years,  
323 contrary to the small pelagic fishes whose BC has still not recovered up to this day (Saraux *et al.*  
324 2019). This study therefore confirms that, as revealed by BC-DFA in trend 2, the impacts of the shift  
325 experienced by the small pelagics in the GOL also affected the demersal system, but without  
326 triggering the same drastic and long-lasting consequences at the biological (for most species),  
327 ecological and economic level.

328 The pelagic community (3 major species of small pelagics) appears to have a strong and lasting  
329 response to the shift, while the demersal community appears to have more diverse responses in both  
330 direction and intensity. Depending on their turnover rates, species respond differently to changes in

the abiotic environment, for example, small pelagic fish that have fast turnover rates react quickly to an abrupt change (Stenseth *et al.*, 2002). Small pelagic fish communities have lower species diversity (Angel, 1993) and are known to have short trophic chains, a short lifespan, and an explosive demography, making them very sensitive to environmental fluctuations (Alheit and Hagen, 2001). Regime shifts were often observed in these communities, like sardines in the California Current (Hill *et al.*, 2015), or anchovies in the Humboldt Current (Guiñez *et al.*, 2014). Conversely, demersal communities often have a greater species diversity (Angel, 1993), live longer and tend to grow slower (Pauly, 1998). They usually display longer trophic chains and are capable of feeding on both benthic and pelagic resources (Garrison and Link, 2000; Bulman *et al.*, 2001). The demersal community food web is therefore generally characterized by higher complexity and modularity, numerous interactions, and these elements are thought to provide a greater stability and inertia to their dynamics (MacArthur, 1955; Paine, 1966; Möllmann and Diekmann, 2012). The difference in responsiveness between small pelagic and demersal systems may explain why the demersal one is usually less affected by environmental changes than the pelagic (Tian *et al.*, 2008; Moyano *et al.*, 2021). It is therefore not surprising that the strong shift signature observed in the small pelagic species of the GOL is only partly mirrored within the demersal community.

The shift period seems to be rather advantageous to cephalopods in terms of their BC. This is particularly interesting as cephalopods are species with a short lifespan that respond very quickly to changing environmental conditions compared to other demersal species (Rodhouse *et al.*, 2014). It has been demonstrated that the increase of water temperature (Mangold, 1983), and the intensification of coastal upwelling (Otero *et al.*, 2016) may have a positive impact on the density and growth of cephalopods and especially the common octopus, as this has been shown in the GOL by Feuilletoy *et al.*, (2020). During the shift, a significant and sudden increase in density was noticed for shortfin squid. Again, the increase of shortfin squid density can be explained by the availability of a favorable environment for the development of cephalopods, such as the rise in the SST (Mangold, 1983) and the intensification of upwellings (Otero *et al.*, 2016) during the mid-2000's.

Identifying the precise drivers of BC changes for each species is beyond the scope of the present study, as it requires further species-centered analyses, that would account for both the effects of fishing and the environment. Depending on the species, these drivers are most likely multiple, and our analysis revealed some degree of inter-specific variability in the temporal patterns, but species of the same taxonomic group tended to exhibit similar patterns. In the absence of knowing what triggered the shift in the GOL, it is difficult to provide a clear explanation for this clustering beyond the fact that taxonomically related species may have more similar physiology, diet and behaviour, and so are more likely to be affected in a similar way by any given change.

On a more general note, the results of the two DFA show that BC time series have more patterns in common across species than density time series. Such an outcome can emerge from a greater sensitivity of BC to common environmental drivers. If the trend 2 on BC time series displays the same patterns of variations as the small pelagic fish and environmental conditions in the GOL, the gradual increase observed in BC (trend 1), to which most species – except cephalopods and anglers – are positively associated, may result from reduced competition among fishes due to increased fishing pressure. Indeed, it is worth pointing out that the drastic response of the small pelagics to the shift led to a collapse of the fishery, the effort of which has been redirected to the demersal stocks. So increased fishing pressure, due to relaxing (perhaps mostly intra-specific) competition, could be one explanation for improved BC in species positively correlated to trend 1.

The objective of the MAR analysis on the hake case study was to determine whether changes in BC may impact population density or vice versa. This analysis displayed the negative effect of the adult density on adult BC, possibly due to intra-specific competition (Hixon and Jones, 2005; Hixon *et al.*, 2012), while adult BC positively affected recruitment, most likely through higher reproductive investment, a better quality of eggs and thus higher recruitment success (Booth and Beretta, 2004; Grote *et al.*, 2011). The search for prey by fish larvae and early fish juveniles, as well as predatory escape, is more efficient in developed individuals (with better BC), assuring that they can overcome the critical larval stage with a better survival rate (Brown and Taylor, 1992; Morgan, 2004). Lloret *et al.* (2008) also confirmed that maternal condition may affect the reproductive potential of hake in the north-western Mediterranean. Interestingly, hake responded positively to trend 1 of the DFA performed on the BC time series and displayed a continuous positive increase in BC while showing a decrease in density. So, the positive link between BC and recruitment suggests that recruitment of the depleted hake population in the GOL can be enhanced through a higher BC in adults, which may be a mechanism that would partly compensate for population decline due to overfishing (GFCM, 2018). The case study of hake clearly demonstrated the importance of investigating the relationship between BC and density for the other species when information is available.

In the MAR analysis on hake, the model was unable to detect the growth of recruits age 0-1 to juveniles age 1-2, and then to adult. This lack of apparent connection between ages 0-1 and 1-2, and ages 1-2 and 2+ has multiple explanations. First, natural mortality in the first year is known to be high and variable (because of changes in environmental conditions) for Teleosts, masking cohort tracking from ages 0-1 (Cushing, 1990). Secondly, the area of distribution of the hake population is wider than the GOL (WGSAD, 2019), so immigration/emigration processes with neighboring areas might be another confounding factor. Thirdly, adult hake are known to take refuge in marine canyons (at the shelf break) and are hence more difficult to track by the MEDITS survey. Still, the model was able

399 to recover a strong positive link between adults' (2+) density and recruits, illustrating that spawning  
400 stock density affects to some extent the recruitment in the following year. Such relationships are often  
401 difficult to observe in fish populations, mostly because recruitment density is more strongly  
402 influenced by environmental variations than spawning biomass (Cury *et al.*, 2014) and because the  
403 low survival rate of recruits is unrelated to the fishing activity. But in cases when the fishing effort  
404 on adults increased beyond a certain threshold (termed recruitment-overfishing by Pauly, 1984;  
405 Sparre and Venema, 1992), stock-recruitment relationships can become more visible in the data,  
406 which is precisely the case for hake in GSA 7 (GFCM, 2018).

407 To summarize, we detected some changes in the BC and density of the demersal species in the GOL  
408 that appeared synchronous with those observed in small pelagic fish populations and in the  
409 environmental conditions of the GOL, but to a lesser extent. We also highlighted strong interactions  
410 between the BC and density in the European hake population, which could partly explain the rather  
411 high resilience of this population to high fishing pressure. This is a good reason to scrutinize  
412 relationships between BC and density for commercial fish stocks.

### 413 **Supplementary material**

414 Supplementary material is available at the ICESJMS online version of the manuscript.

### 415 **Data availability statement**

416 The data underlying this article will be shared on reasonable request to the corresponding author or  
417 to the second author G. Certain ([gregoire.certain@ifremer.fr](mailto:gregoire.certain@ifremer.fr)).

### 418 **Author's contributions**

419 Bensebaini and Certain: conceptualization, methodology, formal analysis, writing and reviewing.  
420 Billet, Jadaud and Hattab: data providing and reviewing. Fromentin and Gourguet: conceptualization  
421 and reviewing.

### 422 **Acknowledgements**

423 We thank Dr M. Hunsicker, and the anonymous reviewers for their helpful suggestions for improving  
424 this manuscript. We also thank Saskia Hampton for her proofreading of this paper. The authors would  
425 like to thank the France Filière Pêche association (FFP) for the financial support of the DEMERSCAN  
426 project. Our gratitude is extended to the AMOP, OP du SUD, and IFREMER members for ensuring  
427 the successful completion of this project.



428 **Table 1.** List of 22 species selected for the DFA analyses with their contribution to the commercial  
429 landings, as well as their estimated density (in number and percentage) in the MEDITS survey catches  
430 of 2018 (study area: Gulf of Lions).

Species	Scientific name	Density (%)	Density (individuals)	Commercial landings (%)
Horned octopus	<i>Eledone cirrhosa</i>	1,38	15263	16.81
Shortfin squid	<i>Illex coindetii</i>	1,54	17010	4.23
Common octopus	<i>Octopus vulgaris</i>	0,19	2109	8.96
Norway lobster	<i>Nephrops norvegicus</i>	0,65	7145	0.13
European hake	<i>Merluccius merluccius</i>	5,62	61943	18.13
Blue whiting	<i>Micromesistius poutassou</i>	2,69	29698	0.11
Greater forkbeard	<i>Phycis blennoides</i>	0,83	9123	0.43
Capelan	<i>Trisopterus capelanus</i>	22,88	252325	10.7
Blackbellied angler	<i>Lophius budegassa</i>	0,72	7970	11.1
Angler	<i>Lophius piscatorius</i>	0,07	746	1.94
Red mullet	<i>Mullus barbatus barbatus</i>	4,78	52751	7.11
Surmullet	<i>Mullus surmuletus</i>	0,09	1038	1.93
Axillary seabream	<i>Pagellus acarne</i>	0,05	502	3.95
Blackspot seabream	<i>Pagellus bogaraveo</i>	0,43	4722	0.7
Common pandora	<i>Pagellus erythrinus</i>	0,37	4103	3.6
Mediterranean horse mackerel	<i>Trachurus mediterraneus</i>	0,35	3905	9.03
Atlantic horse mackerel	<i>Trachurus trachurus</i>	50,63	558400	
Spotted flounder	<i>Citharus linguatula</i>	0,20	2233	0.09
Four-spot megrim	<i>Lepidorhombus boscii</i>	0,32	3522	0.04
Grey gurnard	<i>Eutrigla gurnardus</i>	5,84	64402	0.73
Blackbelly rosefish	<i>Helicolenus dactylopterus</i>	0,35	3861	0.04
John dory	<i>Zeus faber</i>	0,01	103	0.24

432 **Figure 1.** Map of the sampling stations of the MEDITS survey in the Gulf of Lions.

433 **Figure 2.** Process diagram of BC time series extraction.

434 **Figure 3.** Common trends (top part of the figure) for the residual index series obtained by the model  
 435 with two common trends and an “equalvarcov” covariance matrix R, and the factor loadings on these  
 436 trends (bottom part of the figure). The dashed grey lines show the threshold  $\pm 0.2$  (Zuur *et al.*, 2003),  
 437 above which factor loadings will be interpreted.

438 **Figure 4.** Contribution of the two common trends represented in Figure 2 to the fitted series of BC  
 439 of each species. The dotted line represents the effect of the first common trend on each BC time series  
 440 ( $z_{s1}x_{1t}$ ). The dashed line represents the effect of the second common trend ( $z_{s2}x_{2t}$ ). And the solid line  
 441 is the model fit ( $z_{s1}x_{1t} + z_{s2}x_{2t}$ ). Colored points represent the proportion of contributions from each  
 442 trend (example for species  $s$  and trend 1:  $p_{1t} = z_{s1}x_{1t} / (z_{s1}x_{1t} + z_{s2}x_{2t})$ ) to the fit of the models (red for  
 443 trend 1, and blue for trend 2). (a) is the “shift” phase (2006-2009).

444 **Figure 5.** Common trend (top part of the figure) for the density time series obtained by the model  
 445 with one common trend and an “equalvarcov” covariance matrix R, and the factor loadings on this  
 446 trend (bottom part of the figure). The dashed grey lines show the threshold  $\pm 0.2$  (Zuur *et al.*, 2003),  
 447 above which factor loadings will be interpreted.

448 **Figure 6.** Comparison of all common trends obtained by DFA from the current study and the study  
 449 of Feuilloley *et al.* (2020). The dashed line in blue represents BC trend 2 and dotted line in green  
 450 represents density common trend. The brown line with points represents the common trend of small  
 451 pelagics, while the yellow line with diamonds represents the common trend of environmental factors  
 452 from the study of Feuilloley *et al.* (2020). The shaded area of the graph delimits the period for the  
 453 shift between 2006 and 2009.

454 **Figure 7.** Schematic view of the model selected for European hake *M. merluccius*. Red arrows  
 455 represent negative effects, green arrows represent positive effects, arrows with non-significant p-  
 456 value were grayed out.  $x_1$ : recruits age 0-1 log density,  $x_2$ : juveniles age 1-2 log density,  $x_3$ : adults  
 457 age 2+ log density,  $x_4$ : recruits age 0-1 BC,  $x_5$ : juveniles age 1-2 BC,  $x_6$ : adults age 2+ BC.

458 **References**

- 459 Alheit, J., and Hagen, E. 2001. The Effect of Climatic Variation on Pelagic Fish and Fisheries. In  
460 History and Climate: Memories of the Future?, pp. 247–265. Ed. by P. D. Jones, A. E. J.  
461 Ogilvie, T. D. Davies, and K. R. Briffa. Springer US, Boston, MA.
- 462 Angel, M. V. 1993. Biodiversity of the Pelagic Ocean. *Conservation Biology*, 7: 760–772.
- 463 Banaru, D., Mellon-Duval, C., Roos, D., Bigot, J.-L., Souplet, A., Jadaud, A., Beaubrun, P., et al.  
464 2013. Trophic structure in the Gulf of Lions marine ecosystem (north-western Mediterranean  
465 Sea) and fishing impacts. *Journal of Marine Systems*, 111: 45–68.
- 466 Barange, M., Bahri, T., Beveridge, M. C. M., Cochrane, K. L., Funge-Smith, S., and Poulain, F. 2018.  
467 Impacts of climate change on fisheries and aquaculture: Synthesis of current knowledge,  
468 adaptation and mitigation options. FAO Fisheries and Aquaculture Technical Paper No, Rome.  
469 628 pp.
- 470 Barnett, L., and Seth, A. K. 2014. The MVGC multivariate Granger causality toolbox: A new  
471 approach to Granger-causal inference. *Journal of Neuroscience Methods*, 223: 50–68.
- 472 Barraquand, F., Picoche, C., Detto, M., and Hartig, F. 2021. Inferring species interactions using  
473 Granger causality and convergent cross mapping. *Theoretical Ecology*, 14: 87–105.
- 474 Bensebaini, C. M., Billet, N., Certain, G., Jadaud, A., and Le Roy, E. 2019. Growth parameters data  
475 (size and weight) and sexual maturity considering fish, cephalopods and crustaceans of the  
476 Gulf of Lions. SEANOE.
- 477 Bertrand, J. A., Gil de Sola, L., Papaconstantinou, C., Relini, G., and Souplet, A. 2002. The general  
478 specifications of MEDITS surveys. *Scientia Marina*, 66.
- 479 Booth, D. J., and Beretta, G. A. 2004. Influence of recruit condition on food competition and predation  
480 risk in a coral reef fish. *Oecologia*, 140: 289–294.
- 481 Brosset, P., Menard, F., Fromentin, J.-M., Bonhommeau, S., Ulses, C., Bourdeix, J.-H., Bigot, J.-L.,  
482 et al. 2015. Influence of environmental variability and age on the body condition of small  
483 pelagic fish in the Gulf of Lions. *Marine Ecology Progress Series*, 529: 219–231.
- 484 Brosset, P., Lloret, J., Munoz, M., Fauvel, C., Van Beveren, E., Marques, V., Fromentin, J.-M., et al.  
485 2016. Body reserves mediate trade-offs between life-history traits: new insights from small  
486 pelagic fish reproduction. *Royal Society Open Science*, 3: 160202.
- 487 Brown, R. W., and Taylor, W. W. 1992. Effects of egg composition and prey density on the larval  
488 growth and survival of lake whitefish (*Coregonus clupeaformis* Mitchell). *Journal of Fish*  
489 *Biology*, 40: 381–394.
- 490 Bulman, C., Althaus, F., He, X., Bax, N. J., and Williams, A. 2001. Diets and trophic guilds of  
491 demersal fishes of the south-eastern Australian shelf. *Marine and Freshwater Research*, 52:  
492 537–548.

- 493 Burnham, K. P., and Anderson, D. R. 2002. Model selection and multimodel inference: a practical  
494 information-theoretic approach. Springer, New York. 488 pp.
- 495 Certain, G., Barraquand, F., and Gårdmark, A. 2018. How do MAR(1) models cope with hidden  
496 nonlinearities in ecological dynamics? *Methods in Ecology and Evolution*, 9: 1975–1995.
- 497 Cury, P. M., Fromentin, J.-M., Figuet, S., and Bonhommeau, S. 2014. Resolving Hjort's Dilemma:  
498 How Is Recruitment Related to Spawning Stock Biomass in Marine Fish? *Oceanography*, 27:  
499 42–47.
- 500 Cushing, D. H. 1990. Plankton Production and Year-class Strength in Fish Populations: an Update of  
501 the Match/Mismatch Hypothesis. In *Advances in Marine Biology*, pp. 249–293. Ed. by J. H.  
502 S. Blaxter and A. J. Southward. Academic Press.
- 503 FAO. 2018a. FISHSTAT database. <http://www.fao.org/fishery/statistics/software/fishstatj/fr>.
- 504 FAO. 2018b. STATE OF MEDITERRANEAN AND BLACK SEA FISHERIES 2018. General  
505 Fisheries Commission for the Mediterranean, Rome. 172 pp.
- 506 Ferraton, F., Harmelin-Vivien, M., Mellon-Duval, C., and Souplet, A. 2007. Spatio-temporal  
507 variation in diet may affect condition and abundance of juvenile European hake in the Gulf of  
508 Lions (NW Mediterranean). *Marine Ecology Progress Series*, 337: 197–208.
- 509 Ferrer-Maza, D., Lloret, J., Munoz, M., Faliex, E., Vila, S., and Sasal, P. 2014. Parasitism, condition  
510 and reproduction of the European hake (*Merluccius merluccius*) in the northwestern  
511 Mediterranean Sea. *ICES Journal of Marine Science*, 71: 1088–1099.
- 512 Feuilloley, G., Fromentin, J.-M., Stemmann, L., Demarcq, H., Estournel, C., and Saraux, C. 2020.  
513 Concomitant changes in the environment and small pelagic fish community of the Gulf of  
514 Lions. *Progress in Oceanography*, 186: 102375.
- 515 Garrison, L. P., and Link, J. S. 2000. Dietary guild structure of the fish community in the Northeast  
516 United States continental shelf ecosystem. *Marine Ecology Progress Series*, 202: 231–240.
- 517 Geweke, J. F. 1984. Measures of Conditional Linear Dependence and Feedback between Time Series.  
518 *Journal of the American Statistical Association*, 79: 907–915.
- 519 GFCM. 2018. Working Group on Stock Assessment of Demersal Species (WGSAD). FAO, Rome.
- 520 Gould, S. J. 1975. Allometry in primates, with emphasis on scaling and the evolution of the brain.  
521 *Contributions to Primatology*, 5: 244–292.
- 522 Granger, C. W. J. 1969. Investigating Causal Relations by Econometric Models and Cross-spectral  
523 Methods. *Econometrica*, 37: 424–438.
- 524 Grote, B., Hagen, W., Lipinski, M. R., Verheye, H. M., Stenevik, E. K., and Ekau, W. 2011. Lipids  
525 and fatty acids as indicators of egg condition, larval feeding and maternal effects in Cape  
526 hakes (*Merluccius paradoxus* and *M. capensis*). *Marine Biology*, 158: 1005–1017.

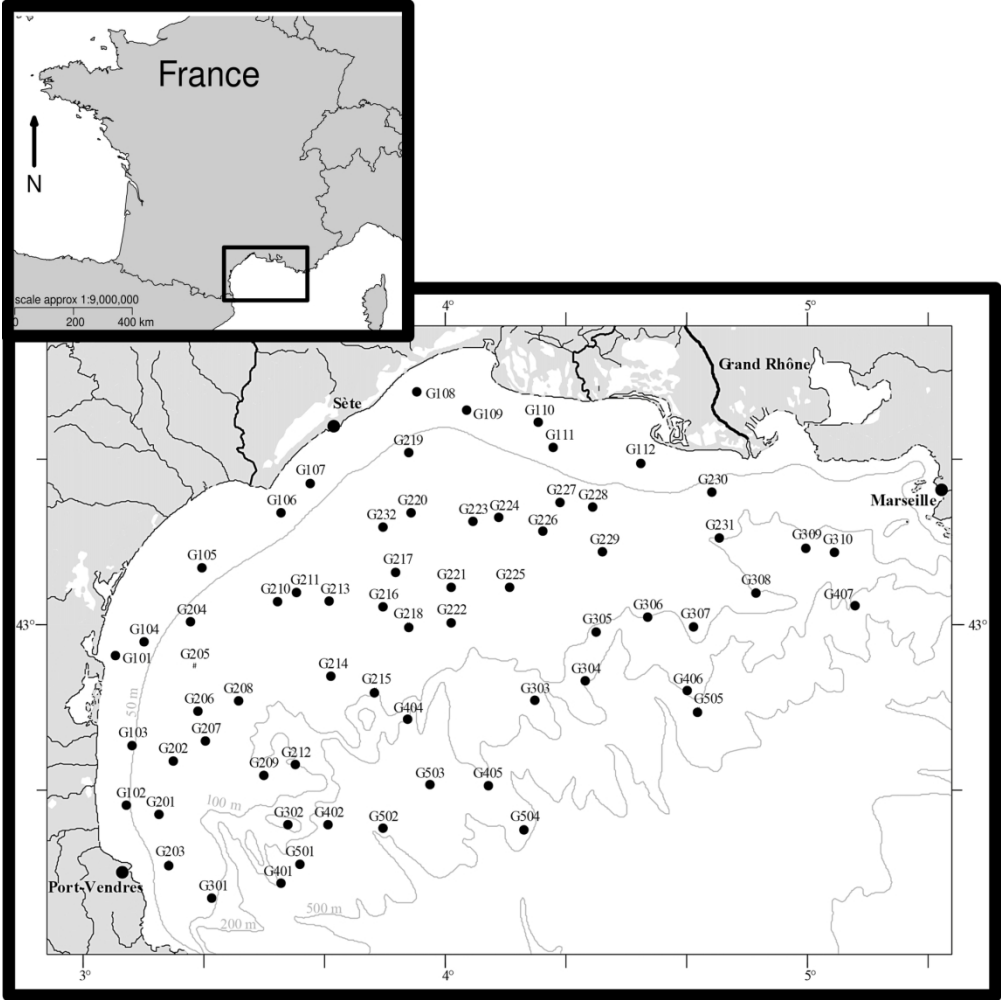
- 527 Guíñez, M., Valdés, J., Sifeddine, A., Boussafir, M., and Dávila, P. M. 2014. Anchovy population  
528 and ocean-climatic fluctuations in the Humboldt Current System during the last 700years and  
529 their implications. *Palaeogeography, Palaeoclimatology, Palaeoecology*, 415: 210–224.
- 530 Harvey, A. C. 1989. *Forecasting, Structural Time Series Models and the Kalman Filter*. Cambridge  
531 University Press. 574 pp.
- 532 Hill, K. T., R., 1958-, C., Paul, Dorval, E., and Macewicz, B. J. 2015. Assessment of the Pacific  
533 sardine resource in 2015 for U.S.A. management in 2015-16.
- 534 Hixon, M. A., and Jones, G. P. 2005. Competition, Predation, and Density-Dependent Mortality in  
535 Demersal Marine Fishes. *Ecology*, 86: 2847–2859.
- 536 Hixon, M. A., Anderson, T. W., Buch, K. L., Johnson, D. W., McLeod, J. B., and Stallings, C. D.  
537 2012. Density dependence and population regulation in marine fish: a large-scale, long-term  
538 field manipulation. *Ecological Monographs*, 82: 467–489.
- 539 Holmes, E. E., Ward, E. J., and Scheuerell, M. D. 2018. Analysis of multivariate time- series using  
540 the MARSS package. Technical report, version 3.10.12. Northwest Fisheries Science Center,  
541 NOAA, Seattle, WA, USA.
- 542 Ives, A. R., Dennis, B., Cottingham, K. L., and Carpenter, S. R. 2003. Estimating Community  
543 Stability and Ecological Interactions from Time-Series Data. *Ecological Monographs*, 73:  
544 301–330.
- 545 Jadaud, A. 1994. MEDITS. <https://doi.org/10.18142/7>.
- 546 Jakob, E. M., Marshall, S. D., and Uetz, G. W. 1996. Estimating Fitness: A Comparison of Body  
547 Condition Indices. *Oikos*, 77: 61–67.
- 548 Jørgensen, T. 1992. Long-term changes in growth of North-east Arctic cod (*Gadus morhua*) and some  
549 environmental influences. *ICES Journal of Marine Science*, 49: 263–278.
- 550 Kooijman, B. (Ed). 2009. Basic concepts. In *Dynamic Energy Budget Theory for Metabolic*  
551 *Organisation*, 3rd edn, pp. 1–23. Cambridge University Press, Cambridge..
- 552 Lambert, Y., and Dutil, J. D. 2000. Energetic consequences of reproduction in Atlantic cod (*Gadus*  
553 *morhua*) in relation to spawning level of somatic energy reserves. *Canadian Journal of*  
554 *Fisheries and Aquatic Sciences*, 57: 815–825.
- 555 Lloret, J., Gil de Sola, L., Souplet, A., and Galzin, R. 2002. Effects of large-scale habitat variability  
556 on condition of demersal exploited fish in the north-western Mediterranean. *ICES Journal of*  
557 *Marine Science*, 59: 1215–1227.
- 558 Lloret, J., Demestre, M., and Sanchez, J. 2008. Lipid (energy) reserves of European hake (*Merluccius*  
559 *merluccius*) in the North-Western Mediterranean. *Vie Et Milieu-Life and Environment*, 58:  
560 77–85.

- 561 MacArthur, R. 1955. Fluctuations of Animal Populations and a Measure of Community Stability.  
562 Ecology, 36: 533–536.
- 563 Mangold, K. 1983. Cephalopod life cycles. London.
- 564 Martinez, M., Guderley, H., Dutil, J. D., Winger, P. D., He, P., and Walsh, S. J. 2003. Condition,  
565 prolonged swimming performance and muscle metabolic capacities of cod *Gadus morhua*. In  
566 Journal of Experimental Biology, pp. 503–511.
- 567 Maynou, F., Lleonart, J., and Cartes, J. 2003. Seasonal and spatial variability of hake (*Merluccius*  
568 *merluccius*) recruitment in the NW Mediterranean. Fisheries Research, 60: 65–78.
- 569 Mellon-Duval, C., De Pontual, H., Metral, L., and Quemener, L. 2010. Growth of European hake  
570 (*Merluccius merluccius*) in the Gulf of Lions based on conventional tagging. Ices Journal Of  
571 Marine Science, 67: 62–70.
- 572 Mellon-Duval, C., Harmelin-Vivien, M., Métral, L., Loizeau, V., Mortreux, S., Roos, D., and  
573 Fromentin, J. M. 2017. Trophic ecology of the European hake in the Gulf of Lions,  
574 northwestern Mediterranean Sea. Scientia Marina, 81: 7–18.
- 575 Millot, C. 1982. Analysis of Upwelling in the Gulf of Lions. In Elsevier Oceanography Series, pp.  
576 143–153. Ed. by J. C. J. Nihoul. Elsevier.
- 577 Millot, C. 1990. The Gulf of Lions' hydrodynamics. Continental Shelf Research, 10: 885–894.
- 578 Möllmann, C., and Diekmann, R. 2012. Chapter 4 - Marine Ecosystem Regime Shifts Induced by  
579 Climate and Overfishing: A Review for the Northern Hemisphere. In Advances in Ecological  
580 Research, pp. 303–347. Ed. by G. Woodward, U. Jacob, and E. J. O’Gorman. Academic Press.
- 581 Morfin, M., Fromentin, J.-M., Jadaud, A., and Bez, N. 2012. Spatio-Temporal Patterns of Key  
582 Exploited Marine Species in the Northwestern Mediterranean Sea. PLOS ONE, 7: e37907.
- 583 Morgan, M. J. 2004. The relationship between fish condition and the probability of being mature in  
584 American plaice (*Hippoglossoides platessoides*). Ices Journal of Marine Science, 61: 64–70.
- 585 Moyano, G., Plaza, G., Cerna, F., and Munoz, A. A. 2021. Local and global environmental drivers of  
586 growth chronologies in a demersal fish in the south-eastern Pacific Ocean. Ecological  
587 Indicators, 131: 108151. Elsevier, Amsterdam.
- 588 Otero, J., Álvarez-Salgado, X., González, Á. F., Souto, C., Gilcoto, M., and Guerra, Á. 2016. Wind-  
589 driven upwelling effects on cephalopod paralarvae: *Octopus vulgaris* and Loliginidae off the  
590 Galician coast (NE Atlantic).
- 591 Paine, R. T. 1969. A Note on Trophic Complexity and Community Stability. The American Naturalist,  
592 103: 91–93.
- 593 Pauly, D. 1984. Fish population dynamics in tropical waters: a manual for use with programmable  
594 calculators. ICLARM Studies and Reviews. 325 pp.
- 595 Pauly, D. 1998. Tropical fishes: patterns and propensities\*. Journal of Fish Biology, 53: 1–17.

- R Core Team. 2020. R: A language and environment for statistical computing. R Foundation for Statistical Computing, Vienna, Austria. <https://www.R-project.org/>.
- Ratz, H. J., and Lloret, J. 2003. Variation in fish condition between Atlantic cod (*Gadus morhua*) stocks, the effect on their productivity and management implications. *Fisheries Research*, 60: 369–380.
- Rodhouse, P. G. K., Pierce, G. J., Nichols, O. C., Sauer, W. H. H., Arkhipkin, A. I., Laptikhovsky, V. V., Lipiński, M. R., et al. 2014. Environmental effects on cephalopod population dynamics: implications for management of fisheries. *Advances in Marine Biology*, 67: 99–233.
- Saraux, C., Van Beveren, E., Brosset, P., Queiros, Q., Bourdeix, J.-H., Dutto, G., Gasset, E., et al. 2019. Small pelagic fish dynamics: A review of mechanisms in the Gulf of Lions. *Deep Sea Research Part II: Topical Studies in Oceanography*, 159: 52–61.
- Sparre, P., and Venema, S. C. 1992. Introduction to tropical fish stock assessment. FAO, Rome. 514 pp.
- STECF. 2019a. EWG 19-10: Stock assessments in the Mediterranean Sea 2019 - Part 1. European Union, Italy.
- STECF. 2019b. EWG 19-16: Stock assessments in the Mediterranean Sea 2019 - Part 2. European Union, Italy.
- Stenseth, N. C., Mysterud, A., Ottersen, G., Hurrell, J. W., Chan, K.-S., and Lima, M. 2002. Ecological Effects of Climate Fluctuations. *Science*, 297: 1292–1296.
- Tian, Y., Kidokoro, H., Watanabe, T., and Iguchi, N. 2008. The late 1980s regime shift in the ecosystem of Tsushima warm current in the Japan/East Sea: Evidence from historical data and possible mechanisms. *Progress In Oceanography*, 77: 127–145.
- Van Beveren, E., Bonhommeau, S., Fromentin, J.-M., Bigot, J.-L., Bourdeix, J.-H., Brosset, P., Roos, D., et al. 2014. Rapid changes in growth, condition, size and age of small pelagic fish in the Mediterranean. *Marine Biology*, 161: 1809–1822.
- Van Beveren, E., Fromentin, J.-M., Rouyer, T., Bonhommeau, S., Brosset, P., and Saraux, C. 2016. The fisheries history of small pelagics in the Northern Mediterranean. *ICES Journal of Marine Science*, 73: 1474–1484.
- Vetter, E. F. 1988. Estimation of natural mortality in fish stocks: a review. *Fishery Bulletin*, 86: 25–43.
- WGSAD. 2019. Working Group on Stock Assessment of Demersal Species (WGSAD) Benchmark session for the assessment of European hake in GSAs 1, 3, 4, 5, 6, 7, 8, 9, 10, 11, 12, 13, 14, 15, 16, 19, 20, 22, 23 and 26 | General Fisheries Commission for the Mediterranean (GFCM) Food and Agriculture Organization of the United Nations. GFCM.

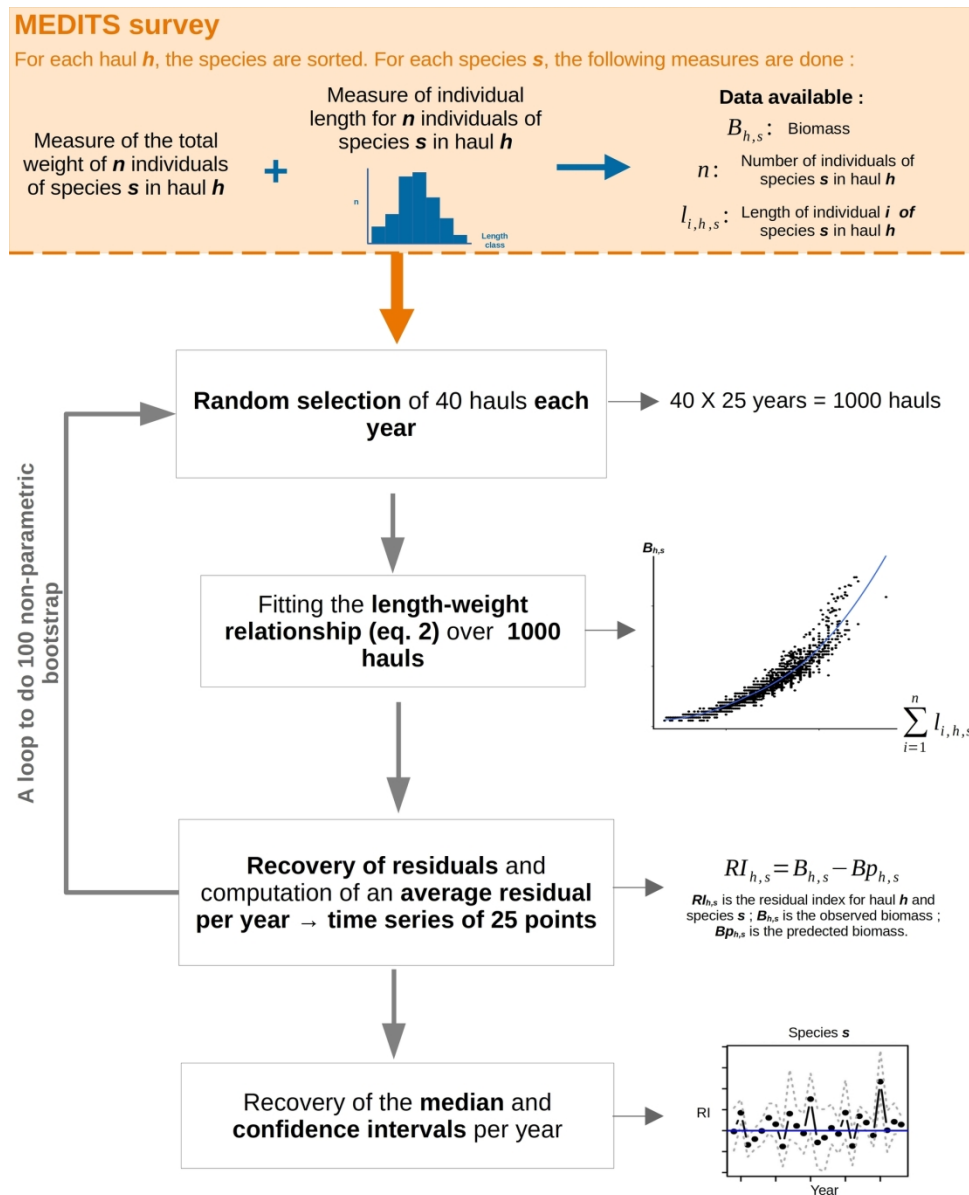
630 Zuur, A. F., Tuck, I. D., and Bailey, N. 2003. Dynamic factor analysis to estimate common trends in  
631 fisheries time series. *Canadian Journal of Fisheries and Aquatic Sciences*, 60: 542–552.





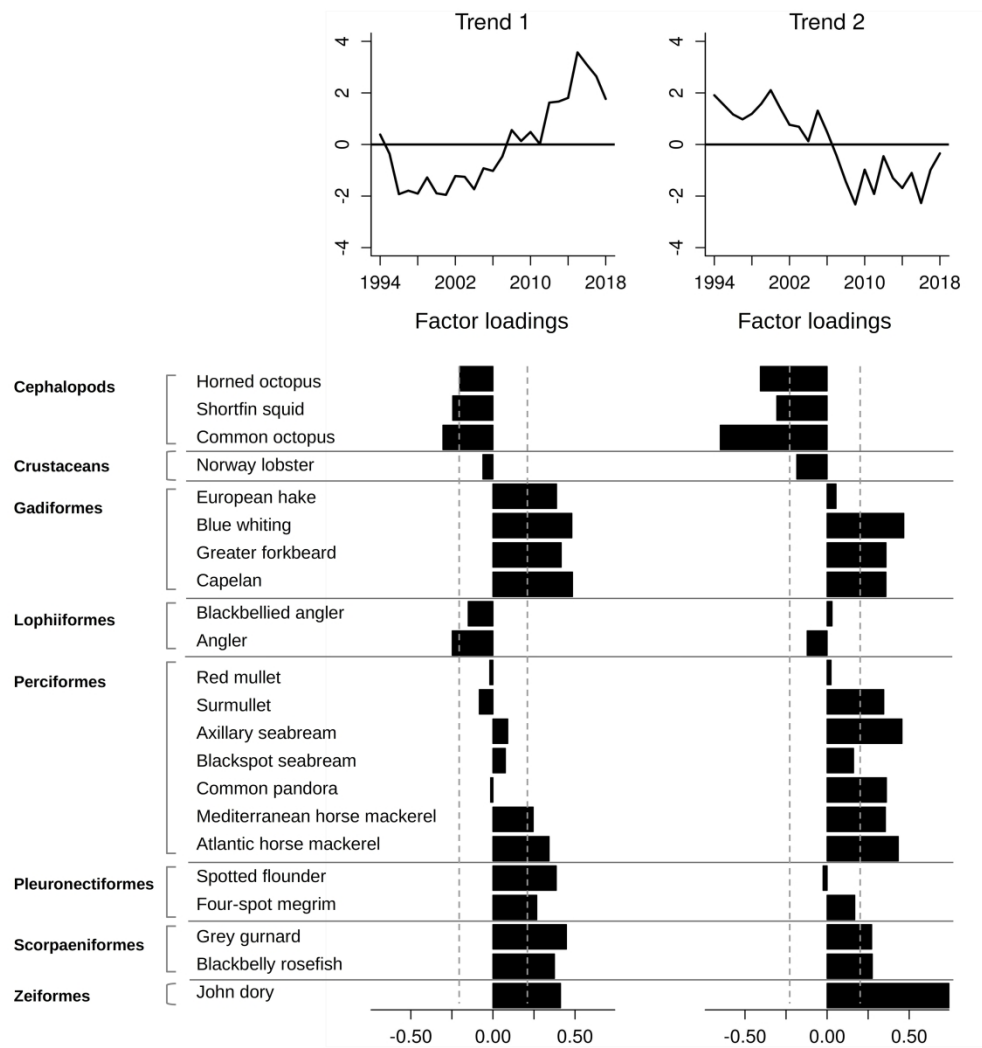
Map of the sampling stations of the MEDITS survey in the Gulf of Lions.

85x85mm (600 x 600 DPI)



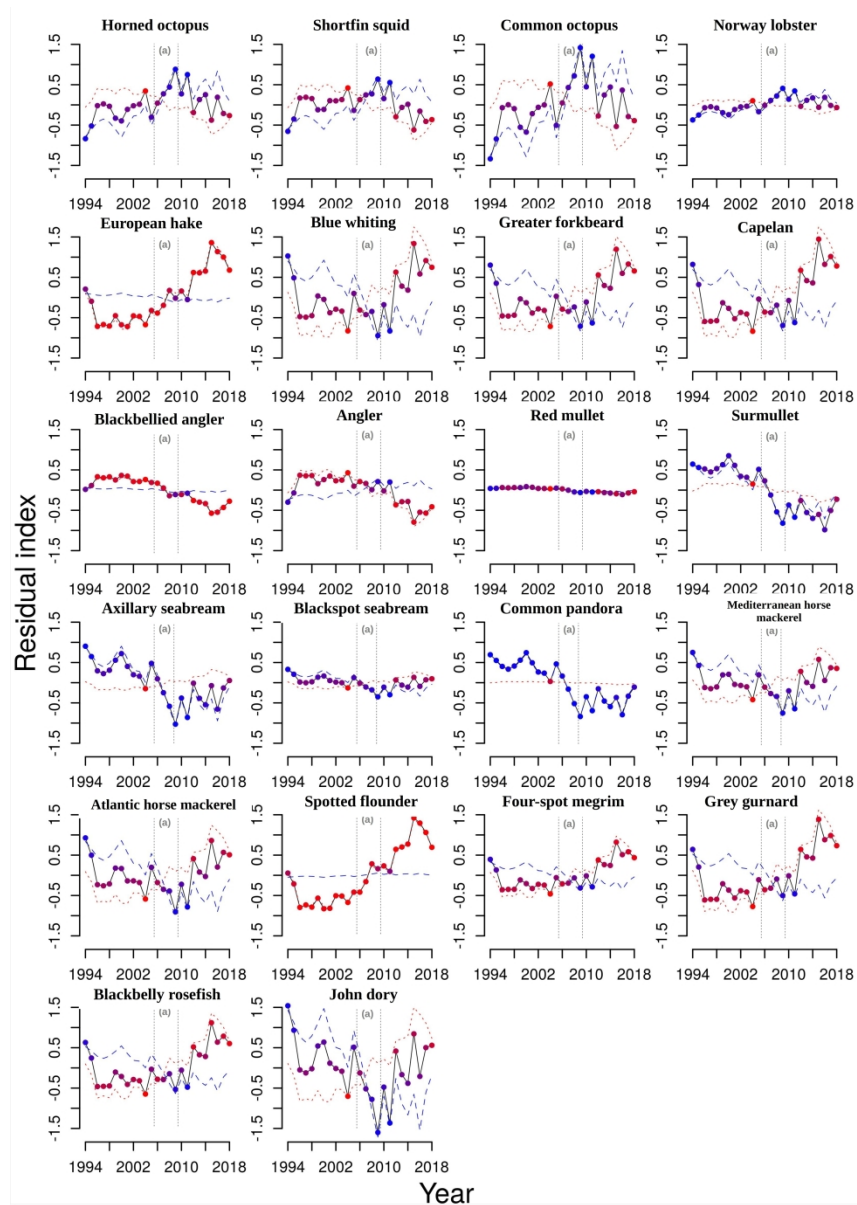
Process diagram of BC time series extraction.

85x105mm (600 x 600 DPI)



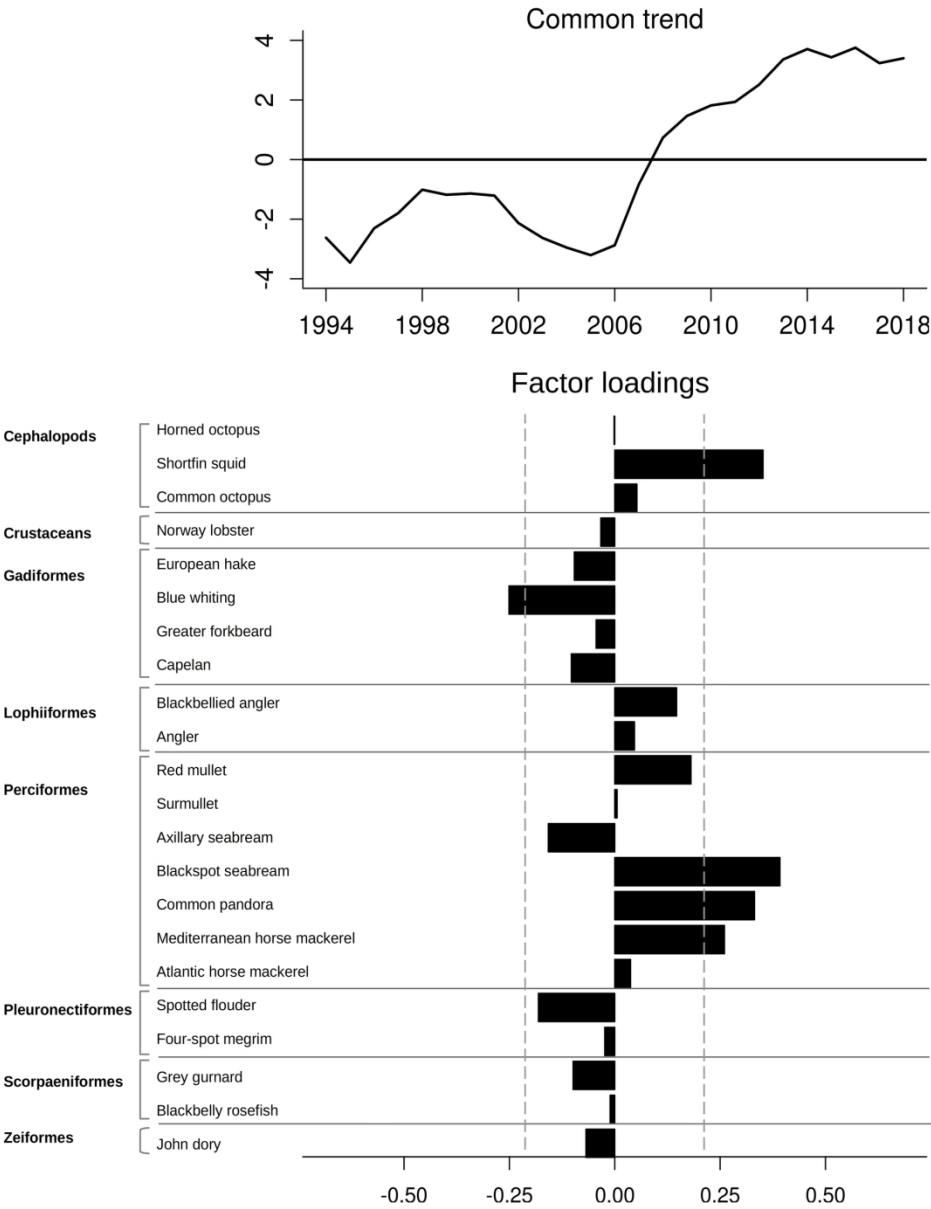
Common trends (top part of the figure) for the residual index series obtained by the model with two common trends and an “equalvarcov” covariance matrix R, and the factor loadings on these trends (bottom part of the figure). The dashed grey lines show the threshold  $\pm 0.2$  (Zuur *et al.*, 2003), above which factor loadings will be interpreted.

170x177mm (600 x 600 DPI)



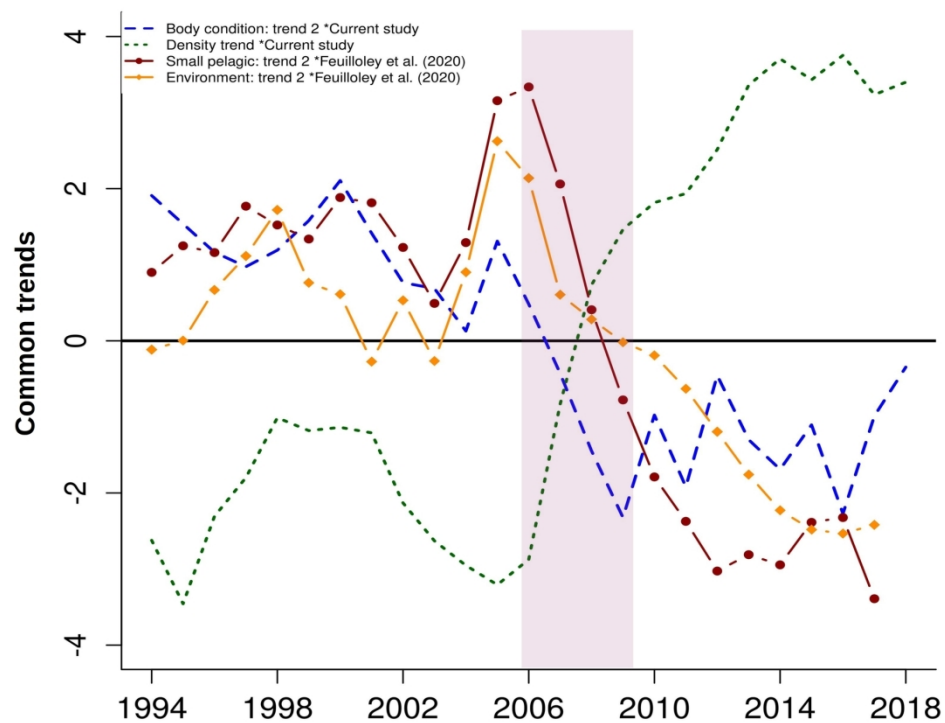
Contribution of the two common trends represented in Figure 2 to the fitted series of BC of each species. The dotted line represents the effect of the first common trend on each BC time series ( $z_{s1} \times 1_t$ ). The dashed line represents the effect of the second common trend ( $z_{s2} \times 2_t$ ). And the solid line is the model fit ( $z_{s1} \times 1_t + z_{s2} \times 2_t$ ). Colored points represent the proportion of contributions from each trend (example for species  $s$  and trend 1:  $p_{1t} = z_{s1} \times 1_t / (z_{s1} \times 1_t + z_{s2} \times 2_t)$ ) to the fit of the models (red for trend 1, and blue for trend 2). (a) is the "shift" phase (2006-2009).

170x240mm (600 x 600 DPI)



Common trend (top part of the figure) for the density time series obtained by the model with one common trend and an “equalvarcov” covariance matrix  $R$ , and the factor loadings on this trend (bottom part of the figure). The dashed grey lines show the threshold  $\pm 0.2$  (Zuur *et al.*, 2003), above which factor loadings will be interpreted.

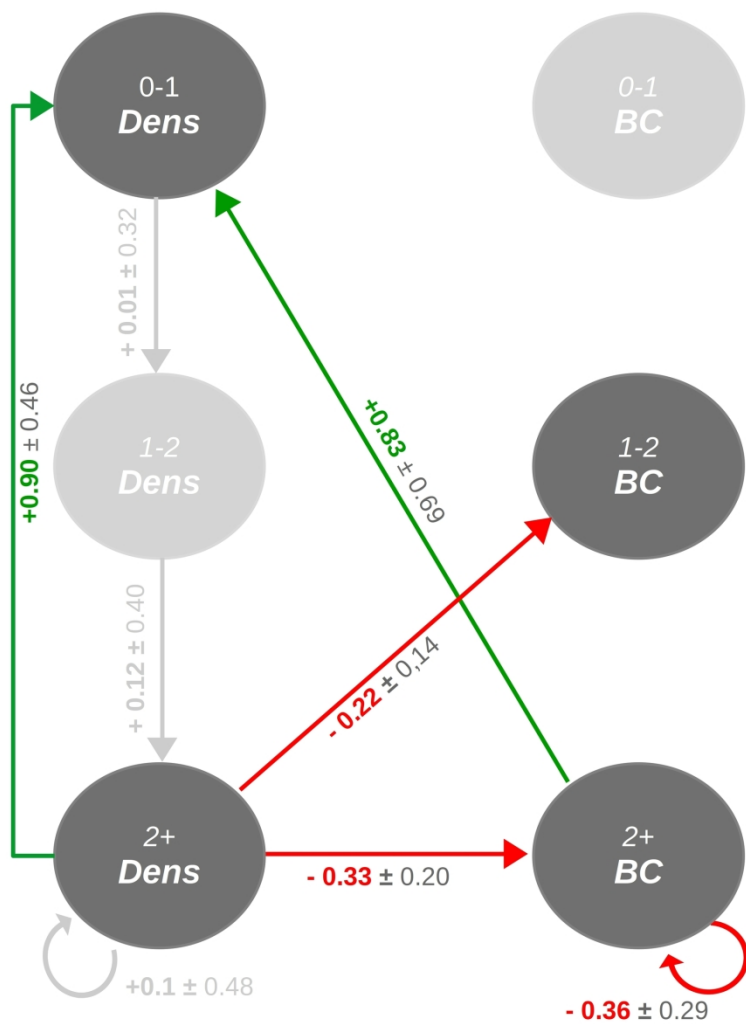
85x105mm (600 x 600 DPI)



Comparison of all common trends obtained by DFA from the current study and the study of Feuilloley *et al.* (2020). The dashed line in blue represents BC trend 2 and dotted line in green represents density common trend. The brown line with points represents the common trend of small pelagics, while the yellow line with diamonds represents the common trend of environmental factors from the study of Feuilloley *et al.* (2020). The shaded area of the graph delimits the period for the shift between 2006 and 2009.

85x68mm (600 x 600 DPI)

European hake



Schematic view of the model selected for European hake *M. merluccius*. Red arrows represent negative effects, green arrows represent positive effects, arrows with non-significant p-value were grayed out.  $x_1$ : recruits age 0-1 log density,  $x_2$ : juveniles age 1-2 log density,  $x_3$ : adults age 2+ log density,  $x_4$ : recruits age 0-1 BC,  $x_5$ : juveniles age 1-2 BC,  $x_6$ : adults age 2+ BC.

85x127mm (600 x 600 DPI)